

## CHAPTER VI

### DISCUSSION

As stated in an introduction Chapter, Southern Kitakami is the very interesting area in Japan having nearly complete sequences of Paleozoic and Mesozoic shallow-shelf facies. Many geologists have tried to figure out the origin of this area. In this study also, the author provided some evidences from petrography and geochemistry of sandstones, together with geochemistry of (detrital) chromian spinels for the interpretation of tectonic settings of the Southern Kitakami area. However, one can argue that there exists some limitation of detrital chromian spinels. To our understanding, although spinels are observed in a great amount in some clastics, many of them cannot be determined for physical and chemical properties due to their fineness or small sizes. The other parameter is that interpretation on physico-chemical result of chromian spinels needs some statistic values to constraint their provenances. This may give rise to the uncertainty if numbers of the results are too small. Therefore, it is unlikely to interpret the result if only a few grains in the samples are encountered. In that case, interpretation has to be treated with a great care, and require a strong support from evidence particularly on classical sedimentological facies (see Chapter III).

#### **6.1 Petrography of sandstones**

Dickinson *et al.* (1983) had proposed the triangular QFL compositional diagram for plotting point counts of sandstones. He subdivided sandstones into fields that one characteristic sandstone-suite derived from different kinds of provenance terranes is controlled by the nature of plate tectonics. Three main classes of provenances were termed as continental blocks, magmatic arcs, and recycled orogens.

Sandstone suites from each include three variants, of which the subfields lie within the larger subdivisions. Average modes of sandstone suites can be classified provisionally according to tectonic setting using the subdivided QFL plots.

Results from the counting of 35 Paleozoic and Mesozoic sandstone samples within the Southern Kitakami area (see Table 4.1) were plotted in this QFL triangular diagram of Dickinson *et al.* (1983) and shown in Figure 6.1. Similar plot of Devonian and Carboniferous sandstones in this area (Kawamura, 1984) are shown in Figure 6.2. Both two plots show similar results, which can be interpreted that tectonic evolution of the Southern Kitakami area had been changed from undissected and transitional arcs in Devonian and Carboniferous to basement uplift in Permian to probably Jurassic.

This interpretation conformed well to the detailed petrographic description of rocks described in Chapter IV. The dominant existing of volcanic lithic fragments, with various sizes and shapes, of Devonian and Carboniferous sandstones suggest that they were transported not so far from the provenance, which could be the arc. And the abundance of plagioclase feldspars in Permian to Cretaceous sandstones indicate also that they were derived from uplifted oceanic or island-arc terranes (see Tucker, 1991).

## 6.2 Geochemistry of sandstones

Major oxides of 12 sandstone samples of Devonian, Permian, Triassic, and Jurassic from the Southern Kitakami area were additionally analysed using XRF technique. With some specific limitations, the results (in Appendix II) were then plotted in diagram between  $\text{Fe}_2\text{O}_3+\text{MgO}$  and  $\text{TiO}_2$  of Bhatia (1983), and diagram between Discriminant function 1 and Discriminant function 2 of Roser and Korsch (1988).

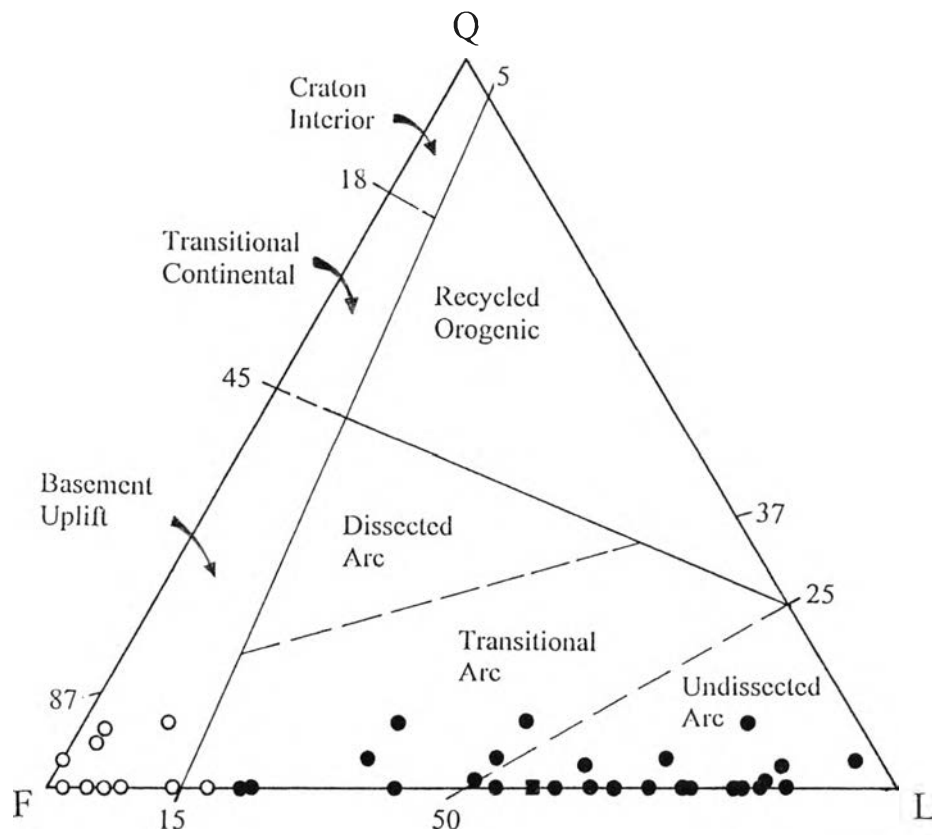


**Figure 6.1** QFL diagram for Devonian (closed square), Carboniferous (closed circles), and Permian to Cretaceous (open circles) sandstones in the Southern Kitakami area. Provenance fields are after Dickinson and others (1983).

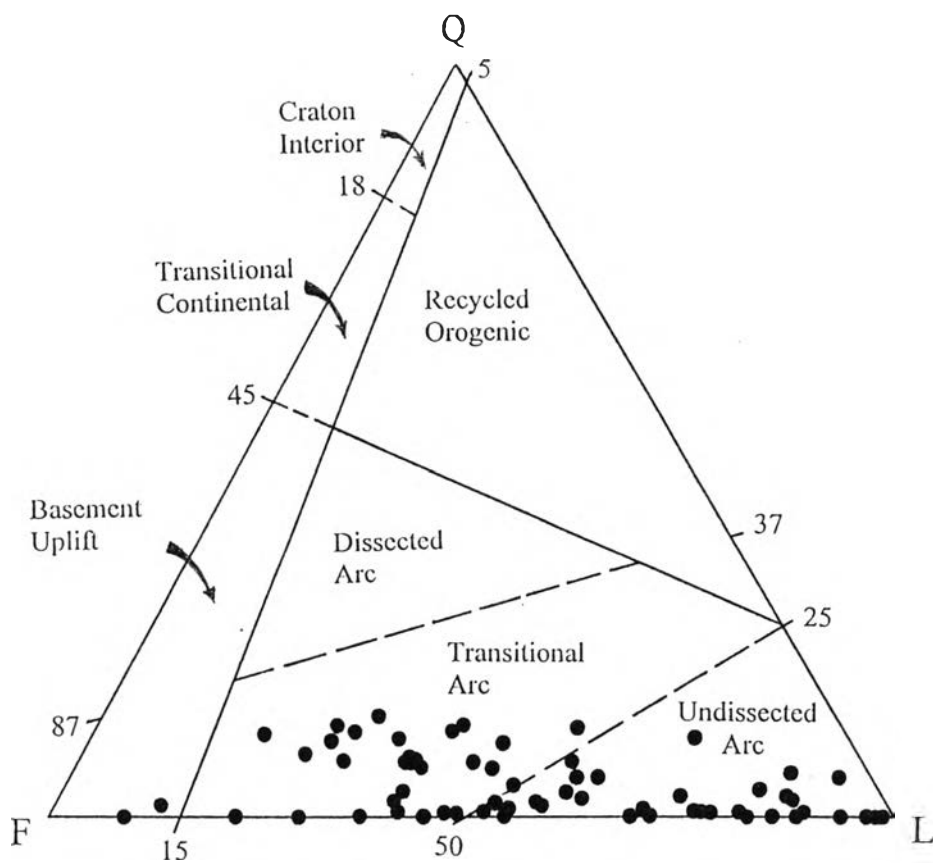


**Figure 6.2** QFL diagram for Devonian and Carboniferous sandstones in the Southern Kitakami area. Provenance fields are after Dickinson and others (1983). Data are from Kawamura (1984).

For diagram between  $\text{Fe}_2\text{O}_3+\text{MgO}$  and  $\text{TiO}_2$ , Bhatia had proposed for the modern sandstones to discriminate among their different tectonic settings. Thus, Devonian sandstone data were scripted, only 8 data of Permian to Jurassic sandstones from this study were plotted in diagram (Fig. 6.3)

In the diagram, two groups of the plots can be observed in different fields of tectonic settings. It can be interpreted from the diagram that the Permian and Triassic sandstones were formed at the oceanic arc while the Jurassic sandstone data from this study indicate the passive margin provenance.

Another discriminant function diagram had been proposed by Roser and Korsch (1988) to distinguish among sediments whose provenance is primarily mafic, intermediate, or felsic igneous and quartzose sedimentary.

All sandstone data were calculated in accordance with the discriminant functions 1 and 2, then plotted against each other in the diagram (Fig. 6.4). The results indicate that these sandstones were derived from felsic and intermediate igneous provenances, which could be arc-regions.

This interpretation gets along well with those of Dozen and Ishiga (1997) who studied the provenances of Permian and Mesozoic shales in the Southern Kitakami area. From their study, intermediate igneous rocks are inferred as the hosts for Permian to Jurassic shales in the area.

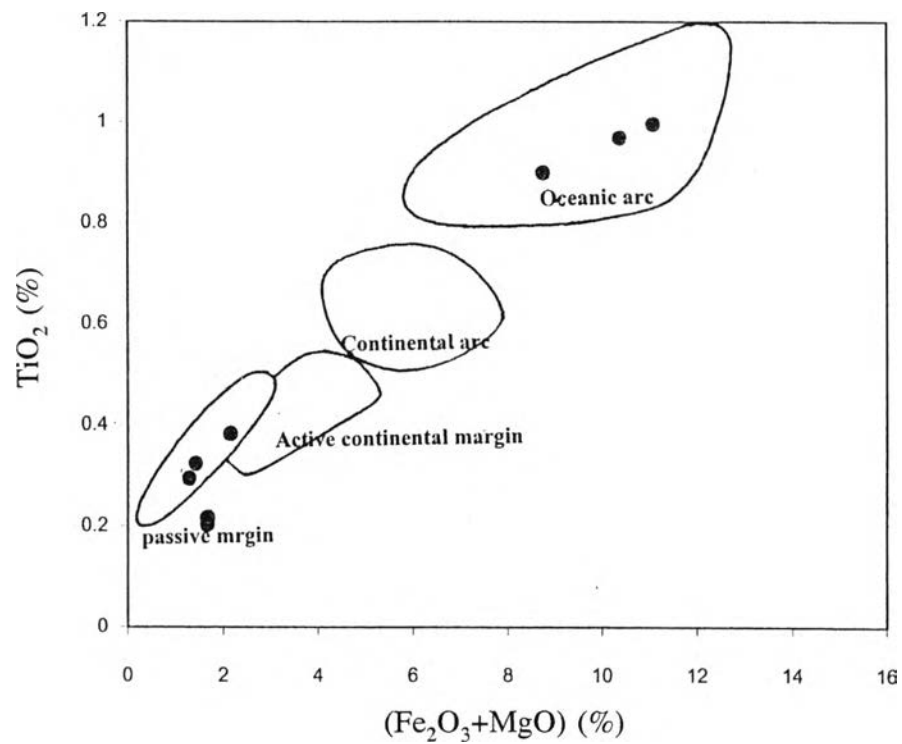


**Figure 6.3** Diagram showing the relationships between Fe<sub>2</sub>O<sub>3</sub>+MgO and TiO<sub>2</sub> of sandstones in the Southern Kitakami area. Provenance fields are after Bhatia (1983).

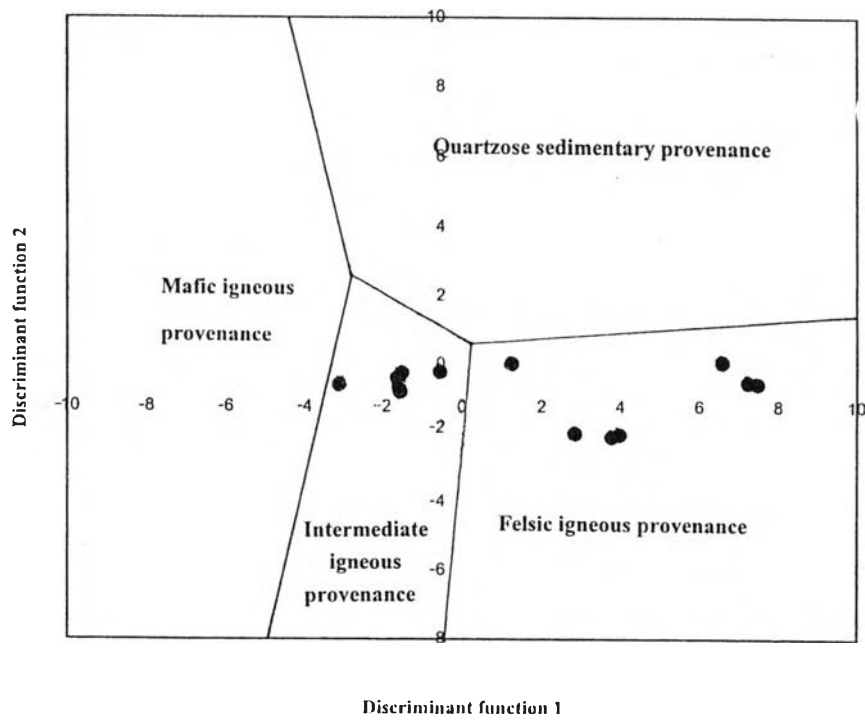


**Figure 6.4** Discriminant function diagram of the provenance signature of sandstones in the Southern Kitakami area. Provenance fields are after Roser and Korsch

(1988). Discrimination function 1 =  $30.638\text{TiO}_2/\text{Al}_2\text{O}_3 - 12.5\text{Fe}_2\text{O}_3/\text{Al}_2\text{O}_3 + 7.329\text{MgO}/\text{Al}_2\text{O}_3 + 12.031\text{Na}_2\text{O}/\text{Al}_2\text{O}_3 + 35.402\text{K}_2\text{O}/\text{Al}_2\text{O}_3 - 6.382$

Discrimination function 2 =  $56.500\text{TiO}_2/\text{Al}_2\text{O}_3 - 10.879\text{Fe}_2\text{O}_3/\text{Al}_2\text{O}_3 + 30.875\text{MgO}/\text{Al}_2\text{O}_3 - 5.404\text{Na}_2\text{O}/\text{Al}_2\text{O}_3 + 11.112\text{K}_2\text{O}/\text{Al}_2\text{O}_3 - 3.89$

### 6.3 Geochemistry of (detrital) chromian spinels

From major oxide values of chromian and detrital chromian spinels shown in Tables 5.2 to 5.4, five interesting cationic ratios listed below were calculated based upon chromian spinel stoichiometry.

$$\text{Cr}^{\#} = \text{Cr}/(\text{Cr}+\text{Al}),$$

$$\text{Mg}^{\#} = \text{Mg}/(\text{Mg}+\text{Fe}^{2+}),$$

$$\text{Al}^{3\#} = \text{Al}/(\text{Cr}+\text{Al}+\text{Fe}^{3+}),$$

$$\text{Cr}^{3\#} = \text{Cr}/(\text{Cr}+\text{Al}+\text{Fe}^{3+}), \text{ and}$$

$$\text{Fe}^{3+3\#} = \text{Fe}^{3+}/(\text{Cr}+\text{Al}+\text{Fe}^{3+}),$$

All Ti was subtracted to form ulvospinel,  $\text{Fe}_2\text{TiO}_4$ , one of the inverse spinels substituting with magnetite (Fig. 5.1).

Petrochemistry of detrital chromian spinels described in the previous chapter, indicate both mafic and ultramafic igneous provenances of the fragmental spinels. Thus, diagrams for spinels from basalts of Arai (1992) and diagram of Dick and Bullen (1984) as well as triangular diagram of Cookenboo *et al.* (1997) for spinels from ultramafic rocks were used.

#### 6.3.1 Plots for basaltic host rocks

In order to comprehend the type of basalt that supplied chromian spinel grains for the clastic rocks, all 33 spinel data were plotted in two diagrams between  $\text{Fe}^{3+}/(\text{Cr}+\text{Al}+\text{Fe}^{3+})$  and  $\text{TiO}_2$ , and between  $\text{Cr}/(\text{Cr}+\text{Al})$  and  $\text{TiO}_2$  (Fig.6.5).

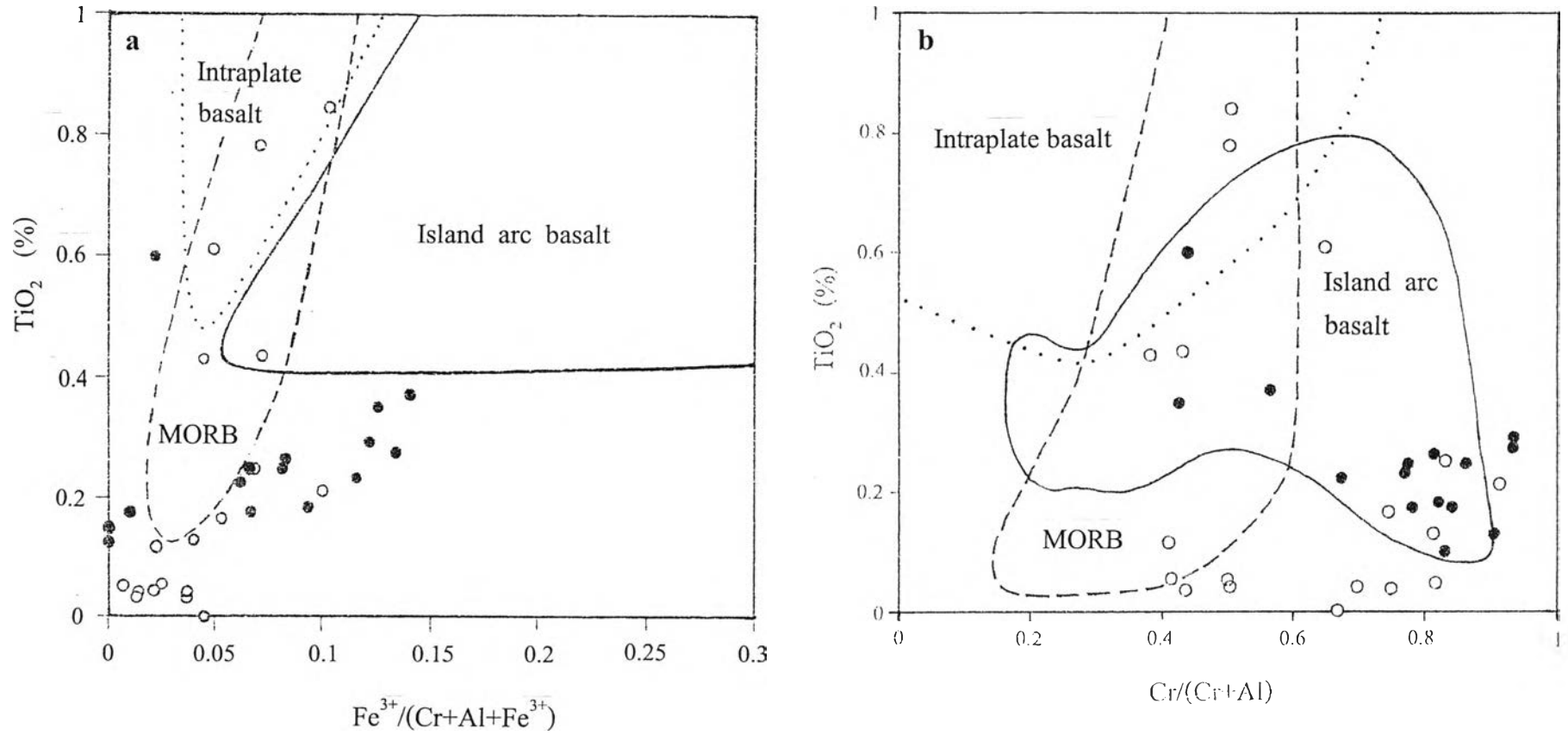


**Figure 6.5** Diagram showing the compositional ratios between (a)  $Fe^{3+}/(Cr+Al+Fe^{3+})$  and  $TiO_2$ , and (b)  $Cr/(Cr+Al)$  and  $TiO_2$  of detrital chromian spinels from Devonian (open circles) and Carboniferous (closed circles) sandstones and siltstones in the Southern Kitakami area. Provenance fields are after Arai (1992).

From the diagram between  $Fe^{3+}/(Cr+Al+Fe^{3+})$  and  $TiO_2$  (Fig. 6.5a), only five grains of Devonian spinels are located in the overlap fields of three basalts. Trend of these five spinels seems to indicate mid-oceanic ridge provenance. Most of the Devonian and Carboniferous spinel-plots are located out of the fields of Arai (1992), however, they seem to have the similar trend with those of Island arc basalt.

In diagram between  $Cr/(Cr+Al)$  and  $TiO_2$  (Fig. 6.5b), some of spinel plots dropped in the mid-oceanic ridge basalt field. However, like the above diagram, many of Devonian and Carboniferous spinels fall within the Island arc basalt field.

Besides the cationic ratio of detrital chromian spinels from the clastic rocks, those of chromian spinel crystals from basalt found in the study area were also plotted in these two diagrams (See Fig.6.6). All the plots of these spinel crystals drop in or with the same trend to an Island arc basalt field.

From these plots, it strongly indicates that Southern Kitakami area had formed on the Island arc since probably Silurian, earlier than Devonian, and continued to the Carboniferous period.

Another way of interpretation, Arai (1994) had summarised the  $Cr/(Cr+Al)$  cationic ratios of chromian spinels at different tectonic settings (Fig. 6.7). When comparing the  $Cr/(Cr+Al)$  cationic ratios of Devonian and Carboniferous detrital chromian spinels from the Southern Kitakami area (Fig. 6.5b) with those of Arai (1994), these detrital minerals should be derived from fore-arc or African Craton.

Comparing the same cationic ratios with those from Carboniferous chromian spinel crystals within the area (Fig. 6.6b), it strongly indicates that basalt containing these chromian spinels had occurred at the fore-arc region.

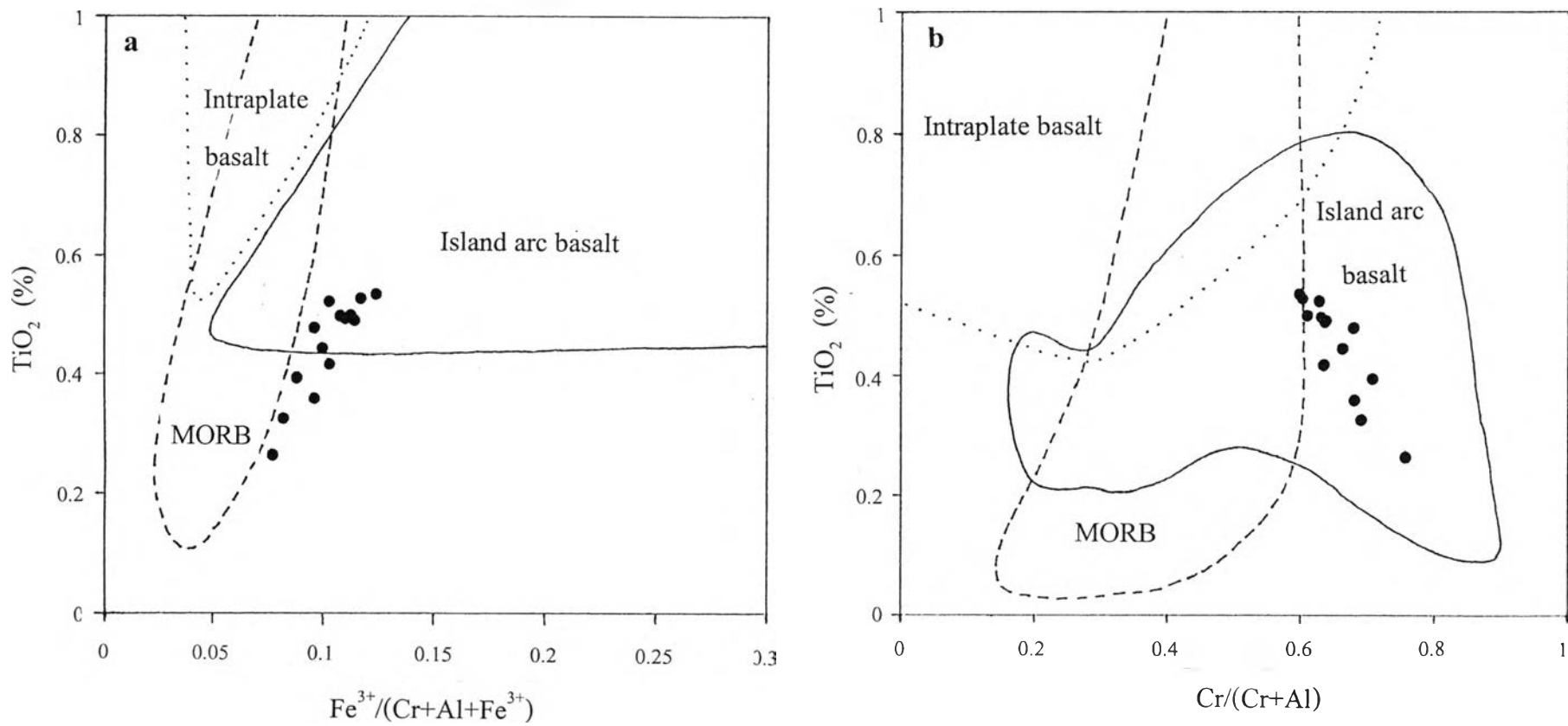


**Figure 6.6** Diagram showing the compositional ratios between (a)  $\text{Fe}^{3+}/(\text{Cr}+\text{Al}+\text{Fe}^{3+})$  and  $\text{TiO}_2$ , and (b)  $\text{Cr}/(\text{Cr}+\text{Al})$  and  $\text{TiO}_2$  of chromian spinels from Carboniferous basalt in the Southern Kitakami area. Provenance fields are after Arai (1992).

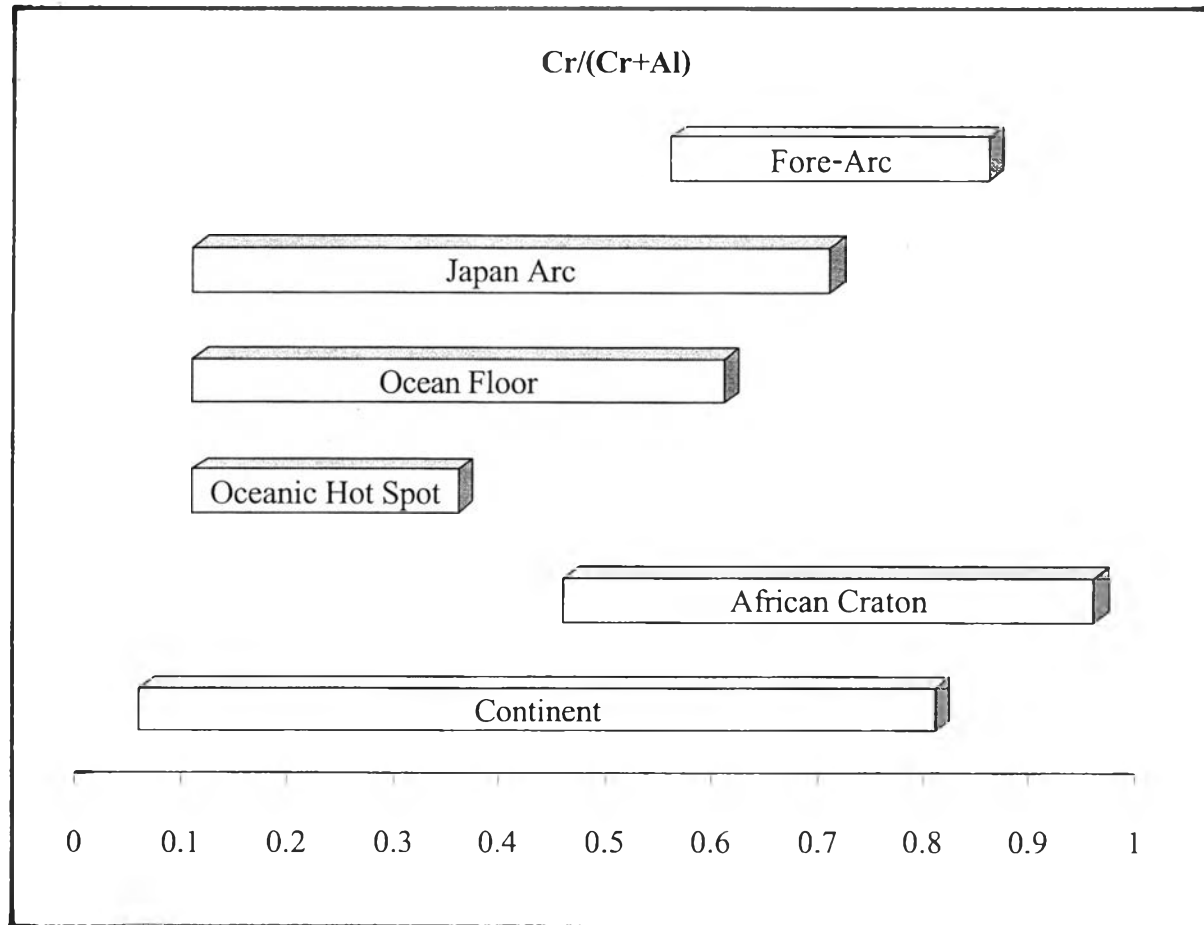


**Figure 6.7** Graph showing the Cr/(Cr+Al) ratio of chromian spinels in various provenances (modified from Arai, 1994).

### 6.3.2 Plots for ultramafic host rocks

Cookenboo *et al.* (1997) had compiled the ultramafic provenance fields for chromian spinels from Alaskan-type complex, Abyssal and Alpine-type peridotites, and Stratiform complexes in  $\text{Fe}^{3+}$ -Cr-Al triangular diagram.

$\text{Fe}^{3+}$ ,  $\text{Cr}^{3+}$ , and  $\text{Al}^{3+}$  of detrital chromian spinels from Devonian and Carboniferous sandstones and siltstones in the Southern Kitakami area were plotted against one another in this triangular diagram (Fig. 6.8). Results from the plots show that Abyssal and Alpine-type peridotites should be the host rocks for these detrital chromian spinels.

Plots of chromian spinels from Miyamori Ultramafic complex of Ozawa (1988) and those from Hayachine Ultramafic complex of Fujimaki and Yomogida (1986) within this  $\text{Fe}^{3+}$ -Cr-Al triangular diagram are compiled and shown in Figure 6.9. These two ultramafic complexes have the  $\text{Fe}^{3+}$ -Cr-Al ratio similar to those of Abyssal and Alpine-type peridotites of Cookenboo *et al.* (1997), and also similar to those of the detrital chromian spinels of this study. Thus, it might be concluded from this similarity that detrital chromian spinels from Devonian and Carboniferous within the Southern Kitakami area probably derived from these two Ordovician ultramafic complexes, which was once located very near each other (Ozawa, 1988).

Another diagram is the relationship between  $\text{Mg}/(\text{Mg}+\text{Fe}^{2+})$  and  $\text{Cr}/(\text{Cr}+\text{Al})$  cationic ratios of Dick and Bullen (1984). They had compiled the ultramafic provenance fields for chromian spinels from S. E. Alaskan Intrusions, Layered Intrusions, Alpine-type peridotites, Abyssal peridotites, and Alpine-type peridotites for chromian spinels. Many overlapping areas among these fields do occur

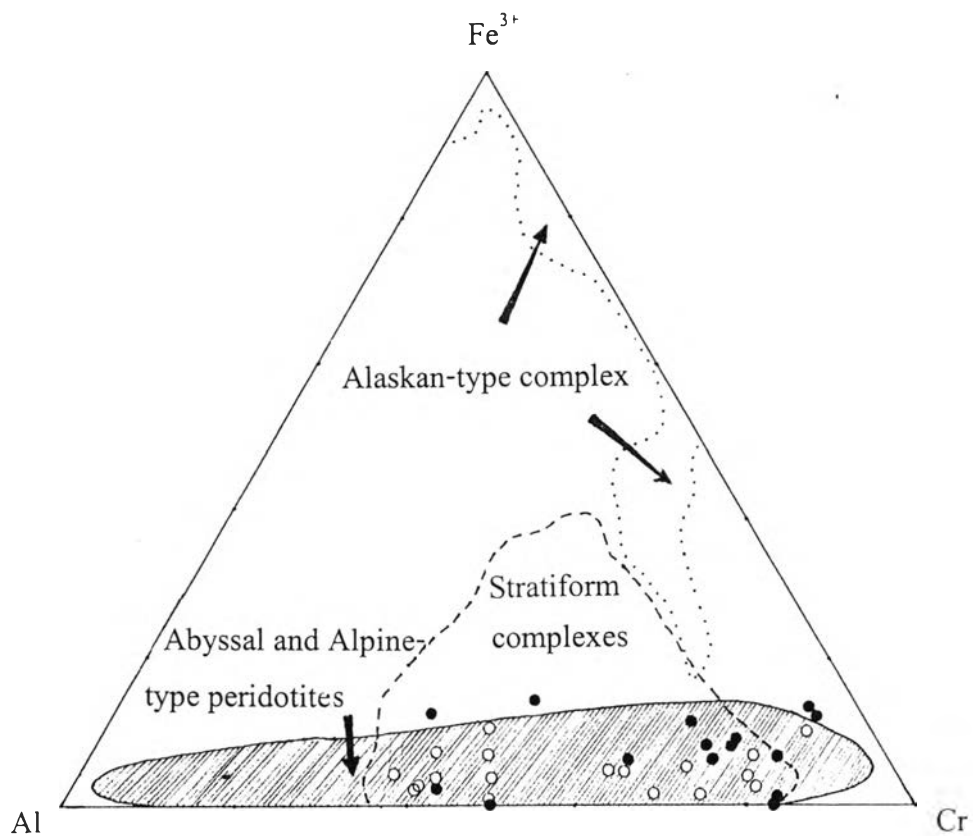


**Figure 6.8**  $\text{Fe}^{3+}$ -Cr-Al triangular diagram showing compositional ratios of detrital chromian spinels from Devonian (open circles) and Carboniferous (closed circles) sandstones and siltstones in the Southern Kitakami area. Host-rock fields are after Cookenboo *et al.* (1997).

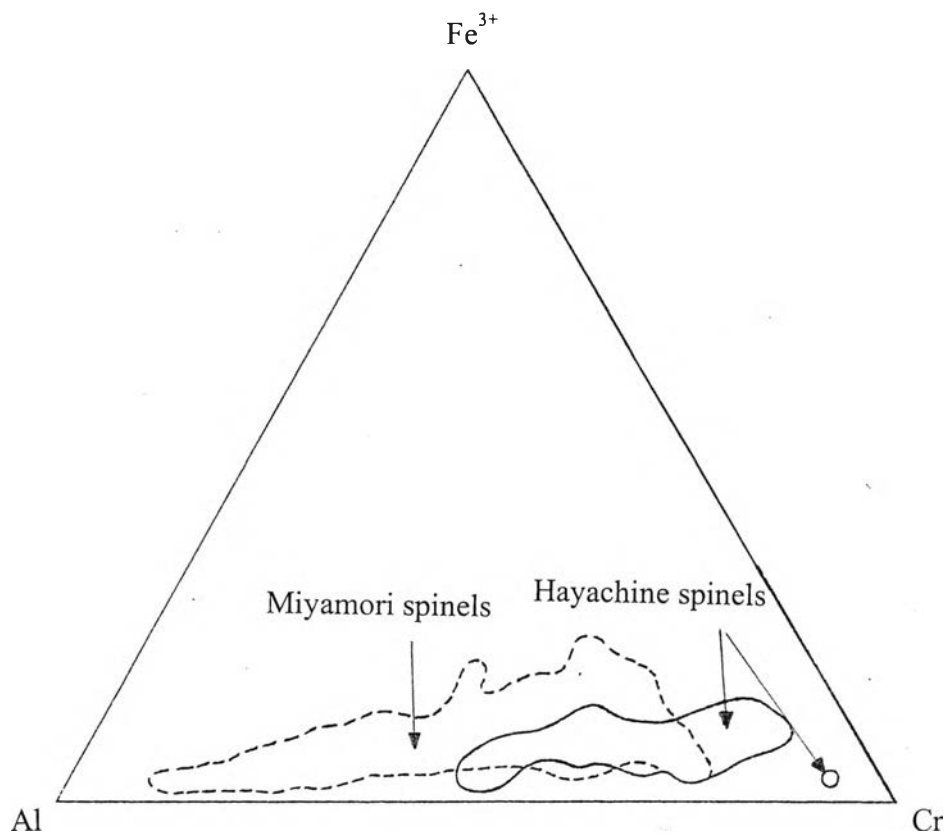


**Figure 6.9**  $\text{Fe}^{3+}$ -Cr-Al triangular diagram showing compositional ratios of chromian spinels from Miyamori (Ozawa, 1988) and Hayachine (Fujimaki and Yomogida, 1986) Ultramafic complexes.

in the diagram. Thus, this diagram should be used carefully together with the other diagrams or data.

Plots between these cationic ratios of detrital chromian spinels from Devonian and Carboniferous clastic rocks within the Southern Kitakami area show slightly wide distribution (Fig. 6.10). Most of them, however, drop within the Alpine-type peridotite conforming to the result in the triangular plot of Cookenboo *et al.* (1997).

Comparing the compositional ratios between  $Mg/(Mg+Fe^{2+})$  and  $Cr/(Cr+Al)$  of detrital chromian spinels from the Southern Kitakami area with those of chromian spinels from various tectonic settings in Figure 6.11 of Huggerty (1991), these ratios are similar to those from the arc (or fore-arc). When comparing these  $Mg/(Mg+Fe^{2+})$  and  $Cr/(Cr+Al)$  cationic ratios with those of Cookenboo *et al.* (1997), Figure 6.12, they are also similar to the ratios of spinels from Island arc. Thus, it can be concluded from these diagrams that detrital chromian spinels from Devonian and Carboniferous strata in the Southern Kitakami area were derived from Alpine-type peridotites below the arc (or fore-arc) region.

#### 6.4 Tectonic scenario of the Southern Kitakami area

Many fossils from Silurian to Early Carboniferous strata (Kimura *et al.*, 1991) in the Southern Kitakami area are similar to those of Yangtze (South China) and Eastern Australia (see Appendix III). These indicate that Southern Kitakami should have been located at the similar environments to Yangtze and Eastern Australia plates in those periods.

Southern Kitakami represents part of the Japanese core which began as a fragment of Gondwanaland (Ehiro and Kanisawa, 1996), or as a segment of the

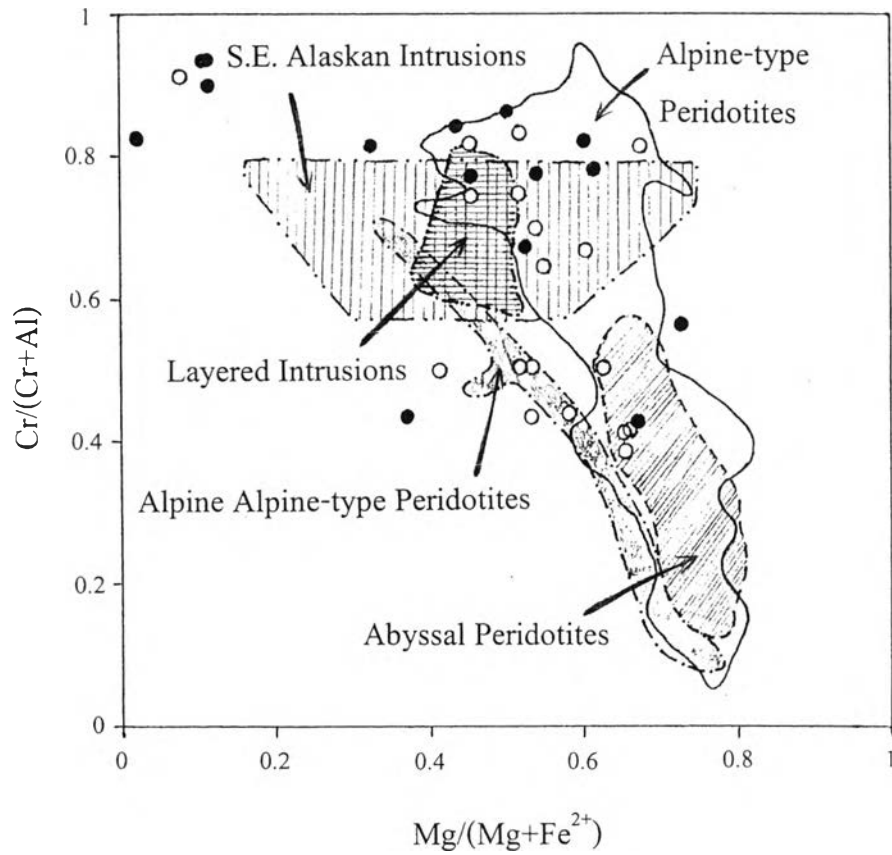


**Figure 6.10** Diagram showing the compositional ratios between  $Mg/(Mg+Fe^{2+})$  and  $Cr/(Cr+Al)$  of detrital chromian spinels from Devonian (open circles) and Carboniferous (closed circles) sandstones and siltstones in the Southern Kitakami area. Host-rock fields are after Dick and Bullen (1984).

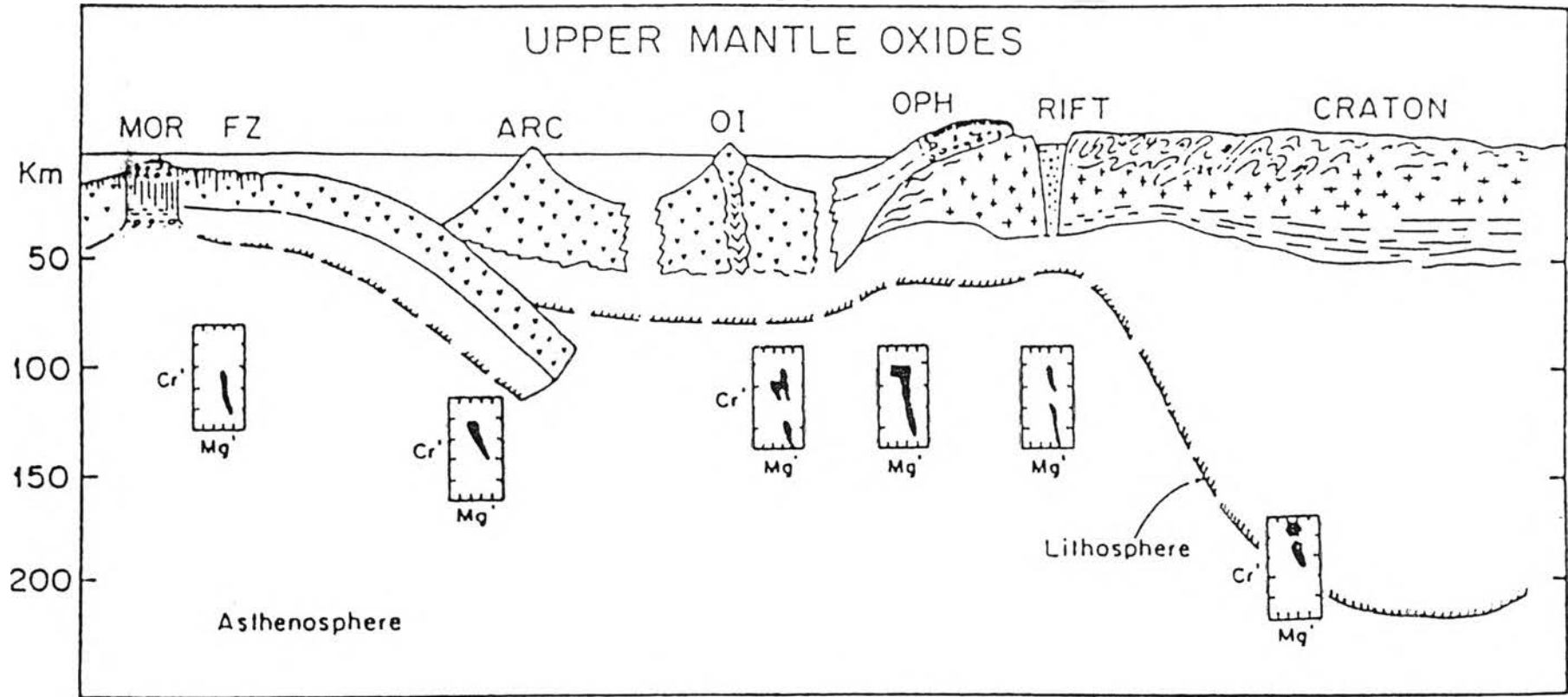


**Figure 6.11** Compositional ratios between Mg'[Mg/(Mg+Fe<sup>2+</sup>)] and Cr'[Cr/(Cr+Al)] of upper mantle oxide minerals in regional tectonic setting from mid-ocean ridge (MOR) and fracture zones (FZ), to arc, ocean islands(OI), ophiolite (OPH) complexes, continental rifts and stable cratons (Haggerty, 1991).

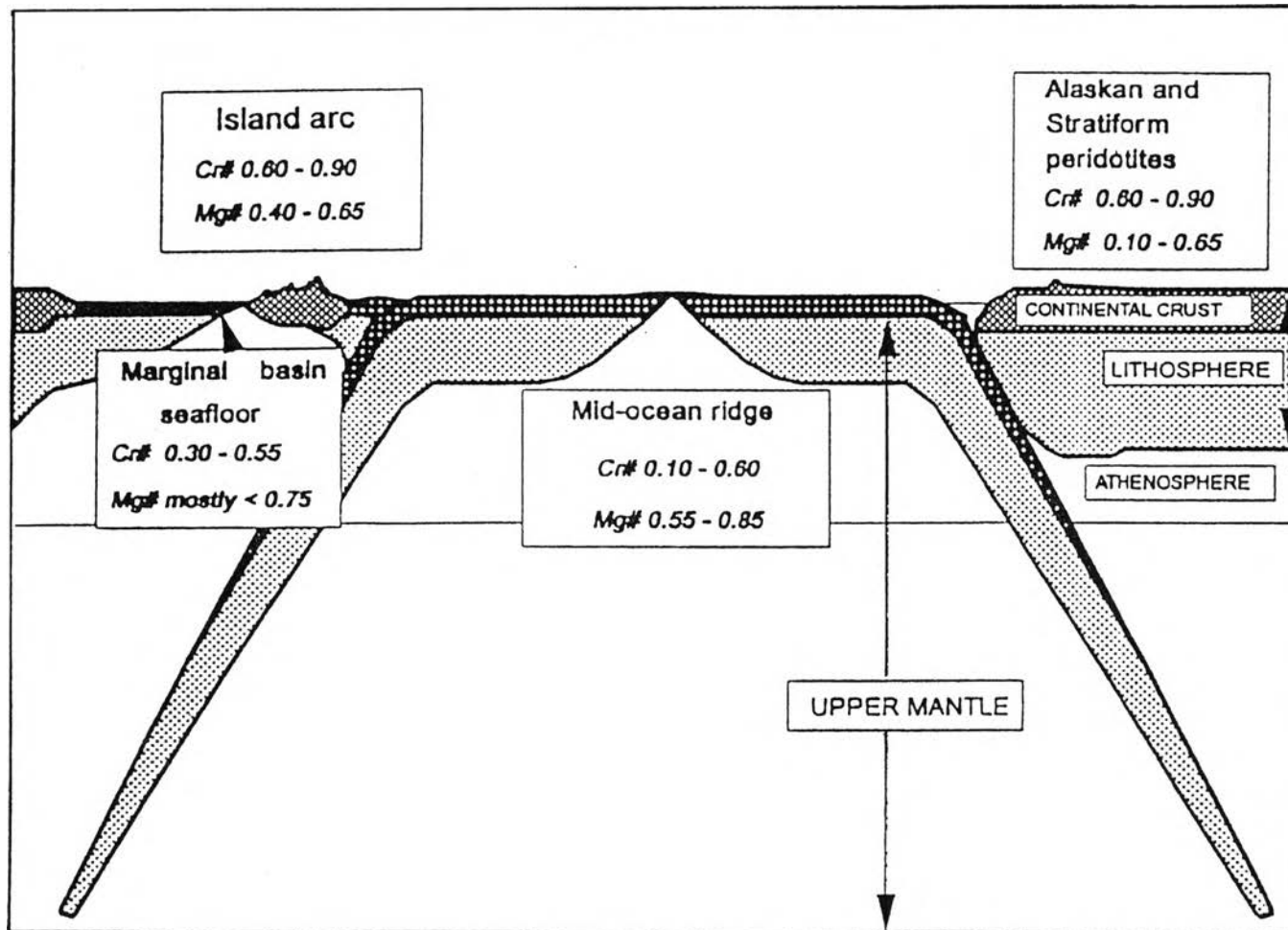


**Figure 6.12** Typical spinel compositions, Cr<sup>#</sup>[Cr/(Cr+Al)] and Mg<sup>#</sup>[Mg/(Mg+Fe<sup>2+</sup>)], from various sea-floor (potential Alpine-type ophiolite) and continental-crust origins (Cookenboo *et al.*, 1997) No scale implied.

Yangtze plate (Isozaki, 1996). Yangtze plate, together with Southern Kitakami, might have been located somewhere close to Australia at the time of at least Silurian from the point of view of fossils (see Appendix III).

This plate began to move northward (Fig. 6.13) as an isolated plate in the Pacific during the Early Devonian (Maruyama *et al.*, 1997). Data from detrital chromian spinels and those from petrography and geochemistry of sandstones indicate that subduction involved in the area of Southern Kitakami all the time during the rifting and drifting events.

In Late Carboniferous (Fig. 6.14), although Yangtze plate containing as a part the Southern Kitakami area was located far away, near the Paleo-Tethys Sea based on coral fauna (see Appendix III), from Australia (Ehiro and Kanisawa, 1996), subduction still occurred based on geochemistry of chromian and detrital chromian spinels and petrography of sandstones.

In Permian, Yangtze and Southern Kitakami had moved passing through the equator into Northern Hemisphere based on the Maiya flora (See Appendix III). Petrography and geochemistry of sandstones in Southern Kitakami area suggest the uplifted basement, which was probably caused by violent subduction.

In Early Triassic, according to Maruyama *et al.* (1997), Yangtze together with Southern Kitakami began to collide with the Sino-Korea (North China), see Figure 6.15. Data from petrography confirmed this collision because many plagioclase feldspars were supplied for the sandstone formation, indicating uplifted basement due to the collision.

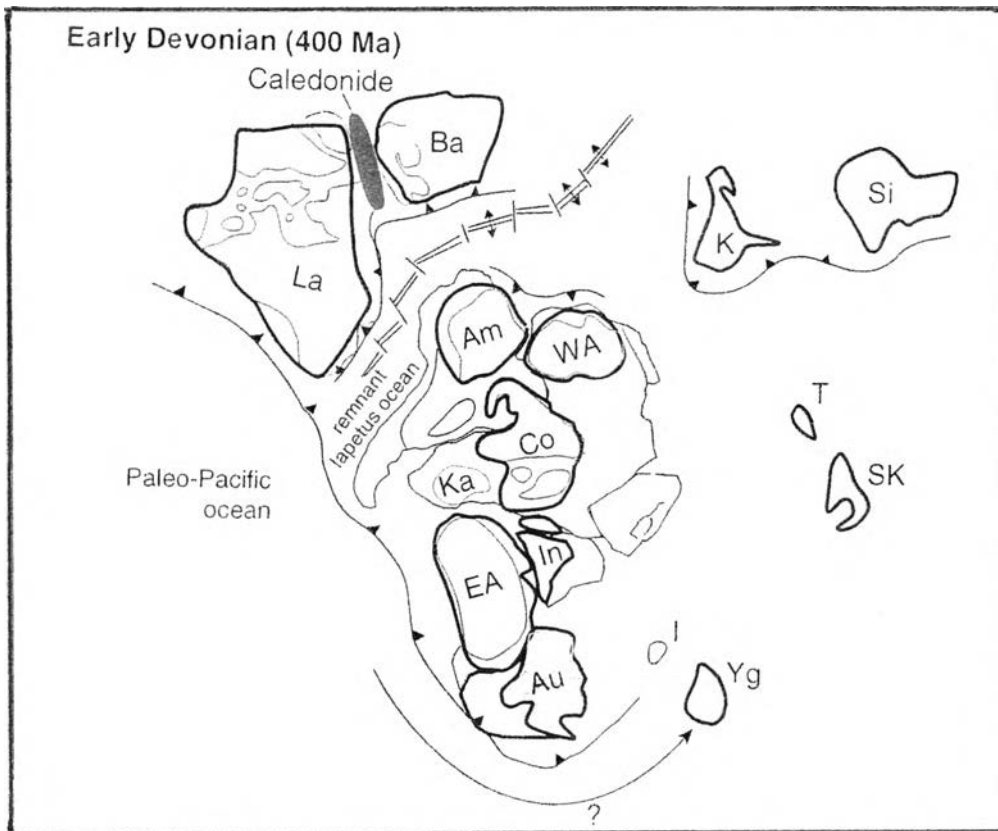


**Figure 6.13** Distribution of the continental blocks in Early Devonian, *ca* 400 M (Maruyama *et al.*, 1997). Yangtze (Yg) together with Southern Kitakami moved northward from Australia (Au) and became an isolated plate in the Pacific Ocean. Sino-Korea (SK) was also isolated from other continental blocks and belong to an independent faunal province.

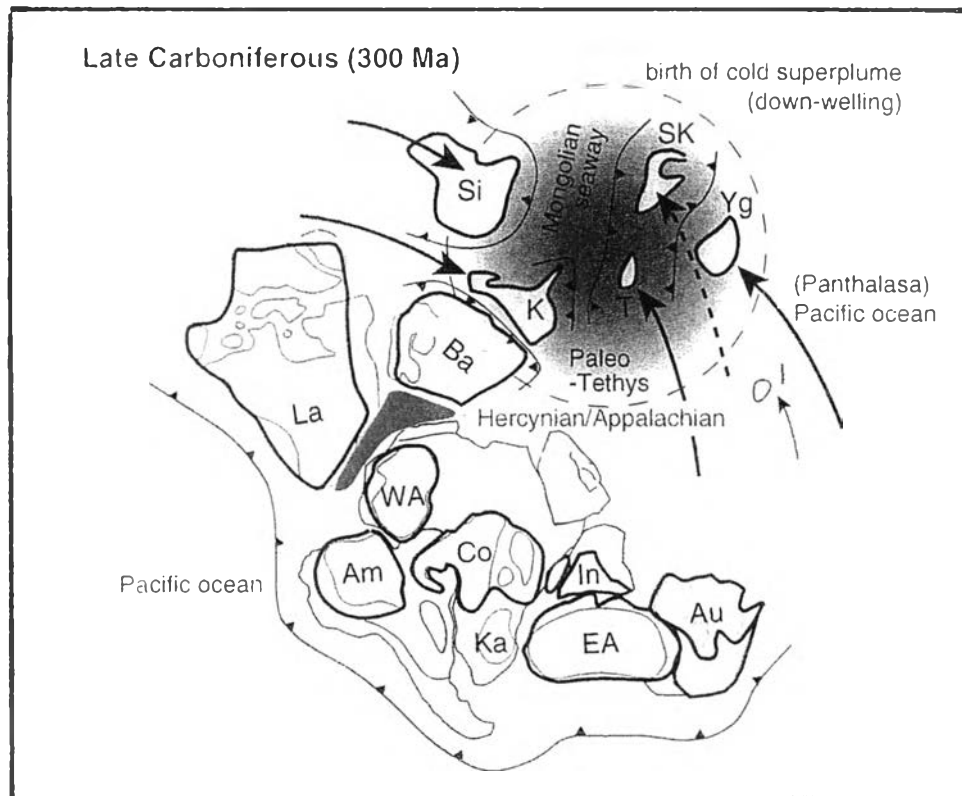


**Figure 6.14** Distribution of the continental blocks in Late Carboniferous, *ca* 300 Ma (Maruyama *et al.*, 1997). Yangtze together with Southern Kitakami and Sino-Korea moved pass the Tethys Sea into the Northern Hemisphere.

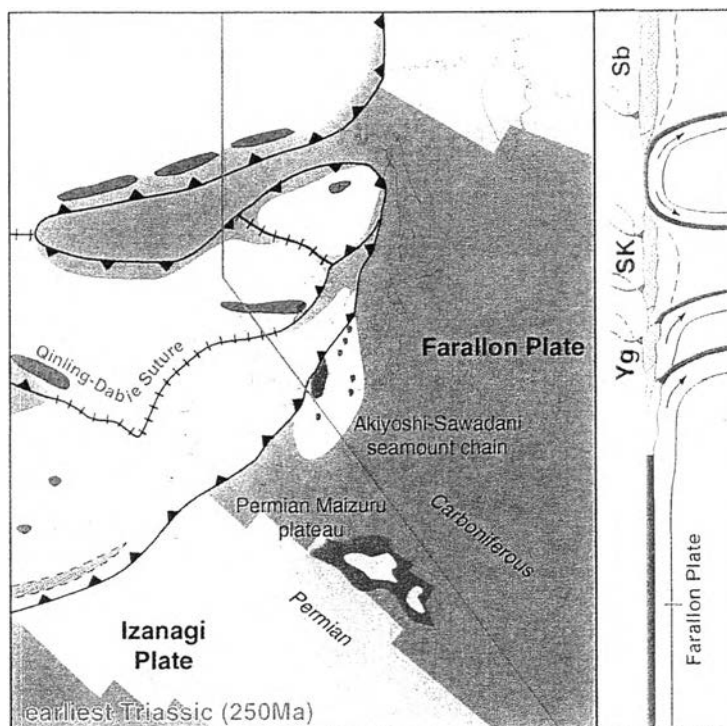


**Figure 6.15** Paleogeographic map of Earliest Triassic Japan at *ca* 250 Ma (Maruyama *et al.*, 1997). Yangtze together with Southern Kitakami started to collide against Sino-Korea close to the Paleo-Tethys seaway.

In Jurassic (Fig. 6.16), strong weathering and erosion of uplifted basements provided abundant sediments to the continental margin (Maruyama *et al.*, 1997). Geochemistry of Jurassic sandstones (Fig. 6.3) indicate the passive margin provenance of those rocks which fits well with the idea of Maruyama (1997) mentioned above.

In summary, several lines of evidences including geochemistry of (detrital) chromian spinels, petrography and geochemistry of sandstones, together with the results from previous investigations (e.g. Maruyama *et al.*, 1997), it can be concluded that Southern Kitakami area had originated at the eastern part of Gondwanaland, with rifting and drifting tectonic settings, by mantle-derived peridotites of the oceanic crust below the fore-arc region, with multiple subduction since at least Silurian to probably Triassic.

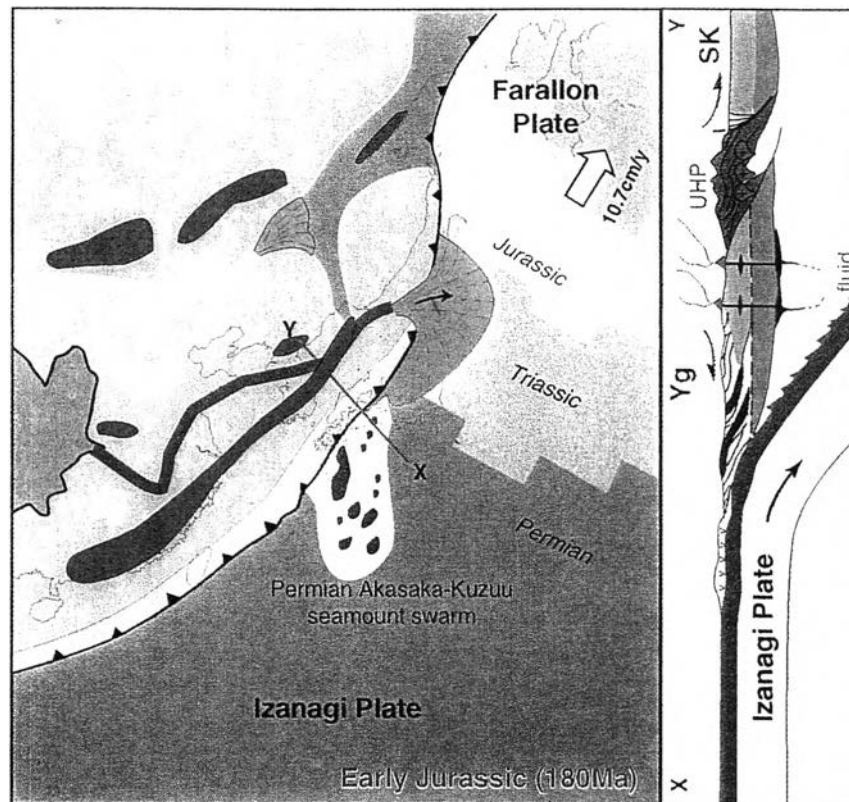


**Figure 6.16** Paleogeographic map of Early Jurassic Japan at *ca* 180 Ma (Maruyama *et al.*, 1997). Violent collision between Yangtze and Sino-Korea caused the uplift of basement, which was then supplied enormous sediments into the marginal continent.